Wide-Area Phasor POD: A New Approach to Handling Time-Varying Signal Latency

Nilanjan Ray Chaudhuri, Balarko Chaudhuri*, Swakshar Ray†, Rajat Majumder‡

*N Ray Chaudhuri and B Chaudhuri are with Imperial College London, London, UK (e-mail: *n.chaudhuri@imperial.ac.uk, b.chaudhuri@imperial.ac.uk*)

†S Ray is with Quanta Technologies, Raleigh, NC, USA (email:*SRay@Quanta-Technology.com*)

‡R Majumder is with ABB Corporate Research, Vasteras, Sweden (e-mail: *rajat.majumder@se.abb.com*)

Abstract

Using present technology, latency associated with remote feedback signals can be determined from the time stamp information at both the PMU location and the control centre. This paper illustrates how this latency could be accounted for in the implementation of a wide-area phasor power oscillation damping controller (phasor POD). The basic idea is to adjust the position of the rotating reference frame - used for phasor extraction - to account for the extra phase shift introduced due to latency. The oscillatory component of the original PMU measurement is retrieved out of the delayed signal received at the control centre. Thus, continuous compensation is achieved without requiring any Pade approximation and/or gain scheduling, unlike the techniques reported in the literature. With the proposed modification, a phasor POD is shown to continuously adapt to the actual latency and maintain the desired dynamic performance over a range of different operating conditions.

1 Introduction

Effectiveness of power oscillation damping (POD) controllers can be improved through use of remote feedback signals [1, 2]. Wide-area measurements systems, increasingly being adopted by utilities these days, does offer such opportunities. However, there is always a risk of latency or delay in communication channels and associated hardware adversely affecting the performance of a wide-area POD [3]. Utilities are concerned about these rare, but probable events of encountering unacceptable delay or even complete loss of signals which could potentially jeopardise the dynamic behaviour of the overall system.

With present technologies, the delay is usually limited to milliseconds, although under unusual circumstances (e.g. congestion in routers etc.) it could go up to hundreds of milliseconds [4, 5] or even more. Such delays, within the range of oscillation frequencies, cannot simply be ignored and should be considered in the control design.

Several ways of tackling the problem of latency have been proposed in the literature [6] being one of the recent ones. Most of them use approximate (e.g. Pade) representation of nominal delay within the system model and design the controller accordingly. An infi-

nite dimensional form of delay was used in [7, 8] along with a predictor based approach. Such fixed controllers, although shown to work 'acceptably' for a range of delays, are usually conservative [9] and produces suboptimal performance under normal scenario. A gain scheduling controller reduces the conservativeness but require the actual latency to be computed for each sample [9]. With accurate time-stamping at both the phasor measurement units (PMU) and the control centre the actual latency associated with each sample can be computed [10], which makes the gain scheduling approach realisable in practice. However, there needs to be a finite number of pre-designed controllers with provision for switching from one to other depending on the actual latency.

In this paper, a new approach to continuous compensation for time varying delay is proposed. Knowledge of computed latency [10] is used in the implementation of a phasor POD [11, 12, 13, 14] - a concept proposed and commercialised by ABB. Kalman filter with random walk matrix instead of the recursive least square (RLS) approach with a scalar forgetting factor [14] is used in this paper. Phasor PODs are already in use in a number of FACTS installations around the world where system operators are interested in exploiting the supplementary damping control feature. In this technique the oscillatory component of a measured signal is extracted in the form of a phasor and an appropriate phase shift is introduced to derive the control signal. However, these PODs have so far relied on locally measured signals (mostly active power flows) where the phase shift requirement for damping could be worked out easily and latency is not a problem. This paper extends the concept to wide-area framework allowing phasor PODs to be more effective which should facilitate their wide-scale deployment in future.

The basic idea behind delay compensation is to adjust the position of the of the rotating reference frame - used for phasor extraction - to account for the phase shift introduced due to latency. The oscillatory component of the original PMU measurement is retrieved out of the delayed signal at the control centre. No Pade approximation and/or gain scheduling is involved unlike most of the techniques reported in the literature. Case studies on a 4-machine, 2-area and also on a 16-machine, 5-area test system confirm that the phasor POD can continuously adapt to the actual latency maintaining the desired dynamic performance over a range of operating conditions.

2 Phasor POD Concept

A Phasor POD visualises the measured signal as a space-phasor (1) which is decomposed into two primary components in a rotating $d-q$ axis reference frame - an oscillatory part corresponding to the dc component and a constant part representing the oscillatory part of the measured signal as shown in (2).

$$S(t) = S_{av} + \mathrm{Re}\{\vec{S}_{ph} e^{j\omega t}\} \tag{1}$$

$$S(t) = S_{av}(t) + S_d(t)\cos\varphi(t) - S_q(t)\sin\varphi(t) \tag{2}$$

where

$$\varphi(t) = \omega t + \varphi_0 \tag{3}$$

The latter is re-transformed back to the stationary reference from the rotating reference frame to extract the oscillatory component of the measured signal in time-domain [11, 12]. The dc and the $d-q$ components are estimated using recursive Kalman filter estimation [15] algorithm. Kalman filter with random walk matrix, although computationally expensive provides more flexibility (degrees of freedom) compared to the recursive least square (RLS) approach with a scalar forgetting factor. Thus the former can adapt better to abrupt changes in operating conditions often encountered in power systems especially, following faults. An overview of the whole methodology is presented in Fig. 1 [13, 12].

Assuming slow-varying $S_d(t)$ and $S_q(t)$, the so-called classical normal equation [15] can be written as:

$$\Phi^T \Phi \Theta = \Phi^T S(t) \tag{4}$$

where the parameter vector (Θ) and the regression matrix (Φ) are given by:

$$\Theta = \begin{bmatrix} S_{av} & S_d(t) & S_q(t) \end{bmatrix}^T \tag{5}$$

$$\Phi = \begin{bmatrix} \phi(t) & \phi(t-T_s) & . & . & \phi(t-NT_s) \end{bmatrix}^T \tag{6}$$

with

$$\phi(t) = [\ 1 \quad \cos\varphi(t) \quad -\sin\varphi(t)\ ] \tag{7}$$

To simplify computation, a recursive estimation approach based on Kalman filters [15] is used here to update the value of $\Theta(t)$ from its previous estimate $\Theta(t-1)$, see (11). The following steps are involved [16]:

Step I: Calculate the prediction error:

$$\varepsilon(t) = S(t) - \phi(t)\Theta(t-1) \tag{8}$$

Step II: Compute the Kalman filter gain vector $K_d(t)$:

$$\mathrm{K}_d(t) = \frac{\wp(t-1)\phi^T(t)}{1 + \phi(t)\wp(t-1)\phi^T(t)} \tag{9}$$

Step III: Update the covariance matrix $\wp(t)$ using random walk:

$$\wp(t) = \wp(t-1) - \mathrm{K}_d(t)\phi(t)\wp(t-1) + R_1 \tag{10}$$

Step IV: Update parameter vector $\Theta(t)$:

$$\Theta(t) = \Theta(t-1) + \mathrm{K}_d(t)\varepsilon(t) \tag{11}$$

Extraction of each mode is facilitated by properly choosing the suitable semi-positive random walk matrix R_1 (see (10)), rather than a conventional forgetting factor used in recursive least square (RLS) techniques, see [15] for more details.

The phase angle of the oscillatory component is derived from $S_d(t)$, $S_q(t)$ which are obtained from updated $\Theta(t)$. Any desired phase shift α can be provided to this signal by changing the relative position of the $d-q$ reference frame with respect to the space-phasor and regenerating a time domain signal in the stationary frame of reference. The required phase shift (assuming positive feedback) is the negative of the phase angle of the open loop system evaluated at the desired closed-loop pole location [17]. Prior knowledge about the frequency of oscillation (ω_0), obtained from the linear model of the system about nominal

condition, is used as the initial frequency for phasor extraction. The dotted box in Fig. 1 shows an online frequency correction loop wherein a PI compensator minimises the error between the phase angles in consecutive samples to correct the frequency. The correction is typically limited to ±0.1 Hz as the POD is not expected to damp oscillations outside this deviation in frequency.

3 Latency Computation from Time-stamp Data

Remote signals are communicated from the PMUs to the control centre through a phasor data concentrator (PDC). A global positioning system (GPS) provides precise timing pulse to correlate the sampled measurements and achieve precise time synchronisation, see Fig. 3. The PDC synchronies the measurements from all the PMUs with microseconds precision and under normal condition, sends data once every 20 ms to the control centre. In case of congestion in one or more channels, the PDC (e.g. PCU400) waits till it receives data from all the PMUs. Therefore, the total latency is the sum of latency in the most congested channel and the time required for synchronisation [10]. Once the PDC receives data from all the channels it starts sending data to control centre at a much faster rate (1 KHz max) until it clears the back-log. During this period the control centre could see feedback signals with time varying latency.

A GPS receiver at the control centre time stamps the signal (with a microseconds precision) received from the PDC. The latency in the communication channel and associated hardware is computed by subtracting the instant of origin at the PMU from that of arrival at the control centre [10]. Thus the state-of-the-art not only provides time stamped measurements but also the latency associated with each sample.

4 Latency Compensation with Adaptive Phase Advance

From a phasor point of view, the latency (T_d) introduces a phase lag in the actual signal with respect to the original measurement at the PMU location. In the proposed approach, the phase lag (θ) is compensated by advancing d-q frame to $d^{'}$-$q^{'}$ through an angle calculated as the product of phasor angular frequency (ω) and time delay (T_d). Thus the phasor

corresponding to the original PMU measurement is retrieved (out of the delayed signal) in the new reference frame as follows, see Fig. 2:

$$\begin{bmatrix} S_d^{'} \\ S_q^{'} \end{bmatrix} = \begin{bmatrix} \cos\omega T_d & -\sin\omega T_d \\ \sin\omega T_d & \cos\omega T_d \end{bmatrix} \begin{bmatrix} S_d \\ S_q \end{bmatrix} \tag{12}$$

Appropriate phase-shift (α) is introduced by further rotating the reference frame to $d^{''}$-$q^{''}$(see Fig. 2) by an angle α to achieve desired damping [11, 13].

$$\begin{bmatrix} S_d^{''} \\ S_q^{''} \end{bmatrix} = \begin{bmatrix} \cos\alpha & -\sin\alpha \\ \sin\alpha & \cos\alpha \end{bmatrix} \begin{bmatrix} S_d^{'} \\ S_q^{'} \end{bmatrix} \tag{13}$$

The shifted phasor in (13) is then transformed back to the corresponding time domain signal to generate the control signal $u(t)$ as in (14), see Fig. 2.

$$u(t) = \begin{bmatrix} \cos\varphi(t) & -\sin\varphi(t) \end{bmatrix} \begin{bmatrix} \cos\alpha & -\sin\alpha \\ \sin\alpha & \cos\alpha \end{bmatrix} \begin{bmatrix} \cos\omega T_d & -\sin\omega T_d \\ \sin\omega T_d & \cos\omega T_d \end{bmatrix} \begin{bmatrix} S_d(t) \\ S_q(t) \end{bmatrix} \tag{14}$$

This control signal $u(t)$ is weighed with appropriate gain and used as the control input for the actuators (e.g. TCSC in this case).

5 Case Study

5.1 Test Systems

Initially, a 4-machine, 2-area system, shown in Fig. 3 [18], is considered to develop an understanding of the challenges. The generators of standard test system are represented by sub-transient models with DC excitation. In steady state, approximately 400 MW flows from area 1 to area 2 over a 220 km transmission line. To control and facilitate a tie-line power flow upto about 800 MW, a TCSC [19] is installed to provide 10% compensation in steady state and has a dynamic range of variation from 1 to 50%. There exists a poorly damped inter-area mode with 0.626 Hz frequency and 1.2 % damping ratio as obtained from the linear model of the system at nominal condition. Further details of the system can be found in [17, 18]. Difference between the phase angles at buses 5 and 11 is used as

the remote feedback signal.

To substantiate the effectiveness of the proposed approach in a relatively complex network, simulation studies are also done with a 16-machine, 5-area test system, see Fig. 4. A detailed description of this study system including machine, excitation system and network parameters can be found in [20]. A PSS connected to one of the generators (generator #9) is tuned to damp two of the three critical inter-area modes. A TCSC, installed on the tie-line connecting the buses 18 and 50, is used to damp the critical inter-area mode with the real power flow in line 16-18 as remote feedback signal.

5.2 Performance with Time-Varying Latency

Scenarios with continuous variation of latency are simulated to demonstrate the performance of the proposed approach. Retrieval of the original PMU measurements out of the delayed signals is shown along with its effect in maintaining satisfactory closed-loop performance in the face of latency. Out of a wide range of scenarios considered for simulation, only a few representative cases are shown below.

Estimation of the original measurement from the delayed signal following a three phase self-clearing fault near bus 8 is illustrated in Fig. 5 under open-loop condition. The latency builds up over two consecutive intervals at t=8 s and t=12 s followed by restoration of the normal scenario (T_d = 25 ms) at t=16 s. During the build up of latency the PDC does not send any new data to the control centre. Some irregularities are observed in the estimated signal during this period due to a constant data input to the phasor estimator. At t=16 s, the delay is restored back to normal (25 ms) prompting the PDC to discard the old data in the queue and send the most recent samples. The overlapping traces confirm that the proposed technique compensates for the phase-lag introduced due to the delay and retrieves the oscillatory component of the original PMU signal.

The effect of delay compensation on the closed-loop damping performance in shown in case of Fig. 6. The latency build up and restoration sequence is identical as in Fig. 5. Sudden fluctuations in TCSC compensation are due to the irregularities in the phasor estimation during the periods of latency build up. It is evident that the phasor POD continuously adapts to the actual latency maintaining the desired dynamic performance.

Fig. 7 shows the damping performance of the phasor POD with a fault near one of the PMU buses (bus 5). The sequence of delays considered is the same as before. The robustness of the phasor POD against faults close to PMU location is evident from this figure. Although not reported, case studies with faults near other buses and different sequences of time-varying latencies revealed that the phasor POD with the proposed modification of delay compensation produces satisfactory damping performance.

5.3 Performance with Lead Compensators

For comparison, lead compensators were designed to achieve desired closed loop performance in presence of signal latency included in the form of Pade approximation within linear system model. As illustrated in Fig. 8, a third order Pade approximation was found to be adequate for delays upto one second. Since a second order approximation introduces considerable phase-shift in the feedback signal at the output of washout block a higher order (third) approximation is suggested. Fig. 9 illustrates the impact of different time delays on the actual settling time (as observed from time domain simulations) with a lead compensator designed for a particular signal latency. It is clear that the performance (in terms of settling time) is compromised not only when the actual latency is larger than the design value, but also for smaller delays. Observations out of a of number of time-domain simulations are summarised in Fig. 9.

5.4 Robustness under Different Operating Conditions

The robustness of the proposed technique is tested under different operating conditions. The tie-line loading is increased from 400 MW to 775 MW and a self-clearing fault is simulated near bus 8. Fig. 10 shows the power flow in the tie-line connecting buses 7 and 8. This figure also compares the TCSC line compensation with and without delay consideration. The lower actuation limit is hit in two consecutive cycles after the fault due to high tie-line flow. While the POD with delay compensation adjusts itself to the variable delay scenario, the one without latency consideration starts violating both the actuation limits. Unlike the previous cases, the limit hitting is sustained even after the latency drops to 25 ms at t = 16 s, deteriorating the damping performance. Similar performance is observed when the

system loading is increased further by 50 MW (see Fig. 11).

To validate the effectiveness of the proposed method under different network configurations, a three-phase fault near bus 8 followed by two different tie-line outage scenarios are simulated. The original remote signal at the PMU location and the measurements at the control centre is illustrated in Fig. 12 after the outage of the tie-line connecting buses 8 and 9. As opposed to the previous results, the latency drops from 1000 ms to 500 ms at t = 16 s and stays there till the end. It can be seen that the system becomes unstable without delay compensation as a result of the persistent signal latency. Also the average power flow through TCSC becomes nearly double due to the outage of a parallel line.

Similar conclusions can be drawn from the simulation results for line 7-8 outage (see Fig. 13). The steady state angular separation between generators 1 and 3 increases due to the increased reactance after the line outage.

5.5 Validation in 16-machine, 5-area System

Having developed in-depth understanding through case studies on the 4-machine, 2-area test system, the proposed technique is tested on a relatively complex system described earlier in Section 5.1.

Fig. 14 shows the system response after a fault near bus 18 followed by the line 18-49 outage (see Fig. 4). At t=8 s, the signal latency builds up to 500 ms, followed by an increase up to 1000 ms at t=12 s and subsequently reverting back to 500 ms again at t=16 s. The effectiveness of the wide-area phasor POD in adjusting to this continuous variation of latency is evident from the system dynamic behaviour in Fig. 14.

Satisfactory damping performance is obtained for a fault near bus 54 and subsequent outage of line 54-53(see Fig. 15). Although not reported here due to space restrictions, faults at different locations with subsequent outages of other key tie-lines confirmed the robustness of this approach.

6 Conclusions

This paper illustrates how the knowledge of signal latency, computed from time-stamp information, can be exploited in countering its adverse impact on power oscillation damping. A conventional phasor POD algorithm is modified to compensate for the phase lag introduced due to latency. The oscillatory component of the original PMU measurement is retrieved out of the delayed signal at the control centre. Hence, continuous compensation is achieved without involving any Pade approximation and/or gain scheduling, unlike the techniques reported in the literature. Case studies on a simple and also a relatively complex test system confirm the effectiveness of the proposed approach for continuously varying latencies over a range of diverse operating conditions.

References

[1] J. Chow, J. Sanchez-Gasca, H. Ren, and S. Wang, "Power system damping controller design-using multiple input signals," *IEEE Control Systems Magazine*, vol. 20, no. 4, pp. 82–90, 2000.

[2] M. Aboul-Ela, A. Sallam, J. McCalley, and A. Fouad, "Damping controller design for power system oscillations using global signals," *IEEE Transactions on Power Systems*, vol. 11, no. 2, pp. 767–773, 1996.

[3] J. W. Stahlhut, T. J. Browne, G. T. Heydt, and V. Vittal, "Latency viewed as a stochastic process and its impact on wide area power system control signals," *IEEE Transactions on Power Systems*, vol. 23, no. 1, pp. 84–91, 2008.

[4] G. Heydt, C. Liu, A. Phadke, and V. Vittal, "Solution for the crisis in electric power supply," *IEEE Computer Applications in Power*, vol. 14, no. 3, pp. 22–30, 2001.

[5] J. Y. Cai, H. Zhenyu, J. Hauer, and K. Martin, "Current status and experience of WAMS implementation in north america," in *IEEE/PES Transmission and Distribution Conference and Exhibition: Asia and Pacific, 2005*, 2005, pp. 1–7.

[6] D. Dotta, A. S. e Silva, and I. C. Decker, "Wide-area measurements-based two-level control design considering signal transmission delay," *IEEE Transactions on Power Systems*, vol. 24, no. 1, pp. 208–216, 2009.

[7] B. Chaudhuri, R. Majumder, and B. Pal, "Wide-area measurement-based stabilizing control of power system considering signal transmission delay," *IEEE Transactions on Power Systems*, vol. 19, no. 4, pp. 1971–1979, 2004.

[8] R. Majumder, B. Chaudhuri, B. Pal, and Q.-C. Zhong, "A unified smith predictor approach for power system damping control design using remote signals," *IEEE Transactions on Control Systems Technology*, vol. 13, no. 6, pp. 1063–1068, 2005.

[9] W. Hongxia, K. S. Tsakalis, and G. T. Heydt, "Evaluation of time delay effects to wide-area power system stabilizer design," *IEEE Transactions on Power Systems*, vol. 19, no. 4, pp. 1935–1941, 2004.

[10] P. Korba, R. Segundo, A. Paice, B. Berggren, and R. Majumder, "Time delay compensation in power system control," European Union Patent EP08 156 785, filed on May 23, 2008.

[11] L. Angquist, "Method and a device for damping power oscillations in transmission lines," U.S. Patent 6 559 561, May 6, 2003.

[12] H. F. Latorre and L. Angquist, "Analysis of TCSC providing damping in the interconnection colombia-ecuador 230 kv," in *IEEE Power Engineering Society General Meeting*, vol. 4, 2003, p. 2366.

[13] L. Angquist and C. Gama, "Damping algorithm based on phasor estimation," in *IEEE Power Engineering Society Winter Meeting*, vol. 3, 2001, pp. 1160–1165.

[14] N. R. Chaudhuri, S. Ray, R. Majumder, and B. Chaudhuri, "A new approach to continuous latency compensation with adaptive phasor power oscillation damping controller (pod)," *to be published in IEEE Transactions on Power Systems.*

[15] P. E. Wellstead and M. B. Zarrop, *Self-tuning Systems. Control and Signal Processing.* John Wiley & Sons, 1991.

[16] K. J. Astrom and B. Wittenmark, *Adaptive control*, 2nd ed. Reading, Mass. ; Wokingham: Addison-Wesley, 1995.

[17] P. Kundur, *Power system stability and control*, ser. The EPRI power system engineering series. New York ; London: McGraw-Hill, 1994.

[18] M. Klein, G. Rogers, and P. Kundur, "A fundamental study of inter-area oscillations in power systems," *IEEE Transactions on Power Systems*, vol. 6, no. 3, pp. 914–921, 1991.

[19] N. G. Hingorani and L. Gyugyi, *Understanding FACTS : concepts and technology of flexible AC transmission systems.* New York: IEEE Press, 2000.

[20] B. Pal and B. Chaudhuri, *Robust control in power systems*, ser. Power electronics and power systems. New York: Springer, 2005.

List of captions

Figure 1 Phasor POD with proposed modification for latency compensation.

Figure 2 Mechanism of latency compensation.

Figure 3 4-machine, 2-area test system with a TCSC. Difference between the phase angles of bus 5 and bus 11 is the feedback signal. Accurate time stamping at the PMU locations and the control centre allows latency to be computed for each sample.

Figure 4 16-machine, 5-area test system with a TCSC. Real power flow between buses 16 and 18 is used as feedback signal.

Figure5 Response with a self-clearing fault near bus 8 (see Fig. 3). Grey trace (upper figure): Remote signal measured at PMU locations. Black trace (upper figure): Remote signal received at the control centre with variable latency (T_d) as marked. Grey trace (lower figure): Oscillatory component of the PMU measurements. Black trace (lower figure): Estimated oscillatory component after delay compensation.

Figure 6 Closed loop system dynamics with a self-clearing fault near bus 8(see Fig. 3). Grey trace (upper figure): Remote signal measured at PMU locations. Black trace (upper figure): Remote signal received at the control centre with variable latency (T_d) as marked. Grey Trace (middle figure & lower figure): response without delay compensation. Black trace (middle figure & lower figure): response with delay compensation.

Figure 7 Damping performance with a self-clearing fault near bus 5 (PMU bus: see Fig. 3). Grey trace (upper figure): Remote signal measured at PMU locations. Black trace (upper figure): Remote signal received at the control centre with variable latency (T_d) as marked. Grey Trace (lower figure): response without delay compensation. Black trace (lower figure): response with delay compensation.

Figure 8 Different Pade order approximations.

Figure 9 Lead compensators designed for desired closed loop performance in presence of

signal latency - modelled by Pade approximation (e.g. Grey trace considers a latency of 250 ms). The effect on the settling time for a range of signal latency is illustrated.

Figure 10 Damping performance with 775 MW tie-line flow after a self-clearing fault near bus 8(see Fig. 3). Grey trace: damping performance without delay compensation. Black trace: response with delay compensation.

Figure 11 Dynamic behaviour with very high system loading (825 MW tie-line flow: see Fig. 3). Grey trace: damping performance without delay compensation. Black trace: response with delay compensation.

Figure 12 Response with fault near bus 8 followed by line 8-9 outage(see Fig. 3). Grey trace (upper figure): Remote signal measured at PMU locations. Black trace (upper figure): Remote signal received at the control centre with variable latency (T_d) as marked. Grey Trace (lower figure): TCSC line power flow without delay compensation. Black trace (lower figure): response with delay compensation. The system is unstable without delay compensation due to a sustained latency of 500 ms.

Figure 13 Damping performance with fault near bus 8 followed by line 7-8 outage(see Fig. 3). Grey trace : response without latency compensation. Black trace : response with delay compensation. The system is unstable without delay compensation due to a sustained latency of 500 ms.

Figure 14 Damping performance with fault near bus 18 followed by line 18-49 outage(see Fig. 4). Grey trace (upper figure): Remote signal measured at PMU locations. Black trace (upper figure): Remote signal received at the control centre with variable latency (T_d) as marked. Grey Trace (lower figure): response without delay compensation. Black trace (lower figure): response with delay compensation.

Figure 15 Damping performance with fault near bus 54 followed by line 54-53 outage(see Fig. 4). Grey trace: response without latency compensation. Black trace: response with delay compensation.

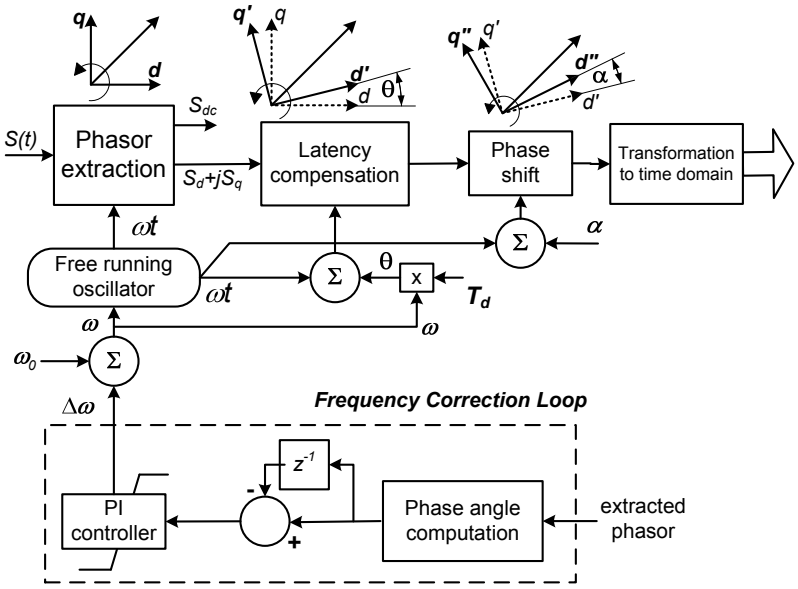

Figure 1: Phasor POD with proposed modification for latency compensation.

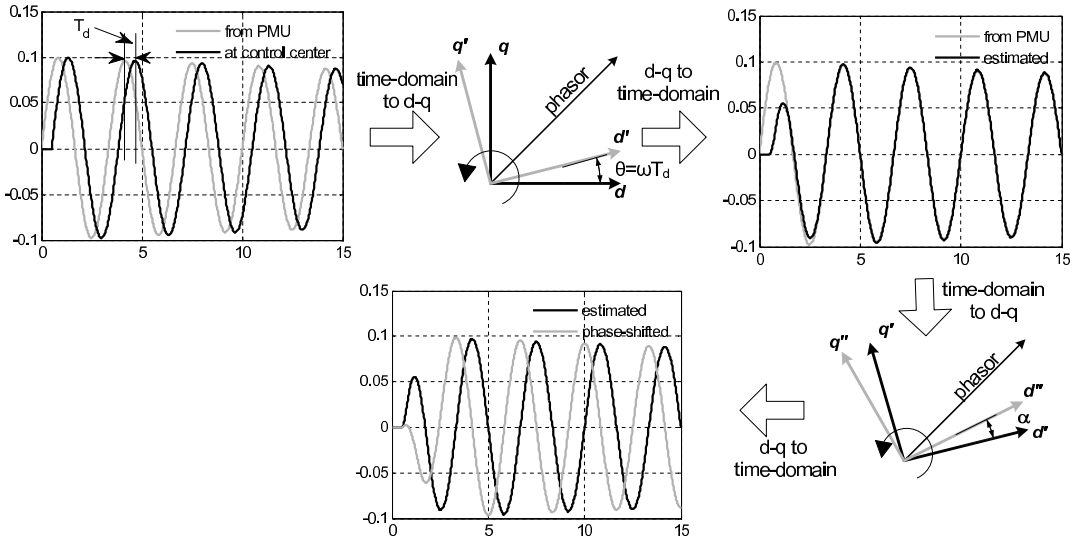

Figure 2: Mechanism of latency compensation

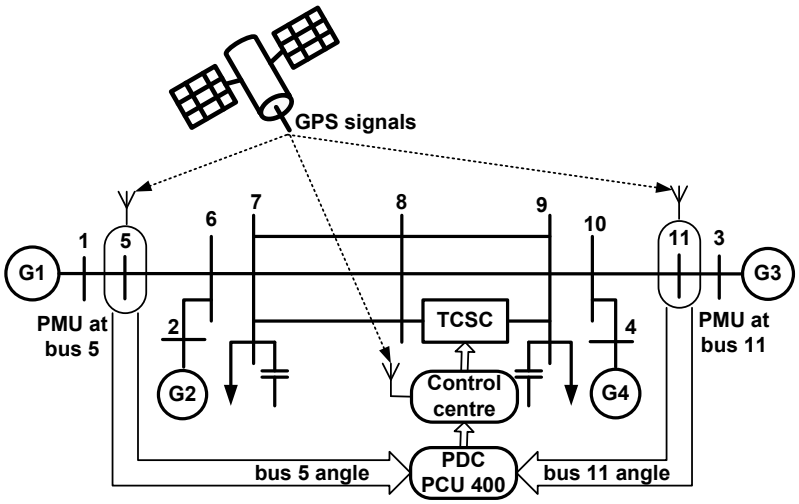

Figure 3: 4-machine, 2-area test system with a TCSC. Difference between the phase angles of bus 5 and bus 11 is the feedback signal. Accurate time stamping at the PMU locations and the control centre allows latency to be computed for each sample.

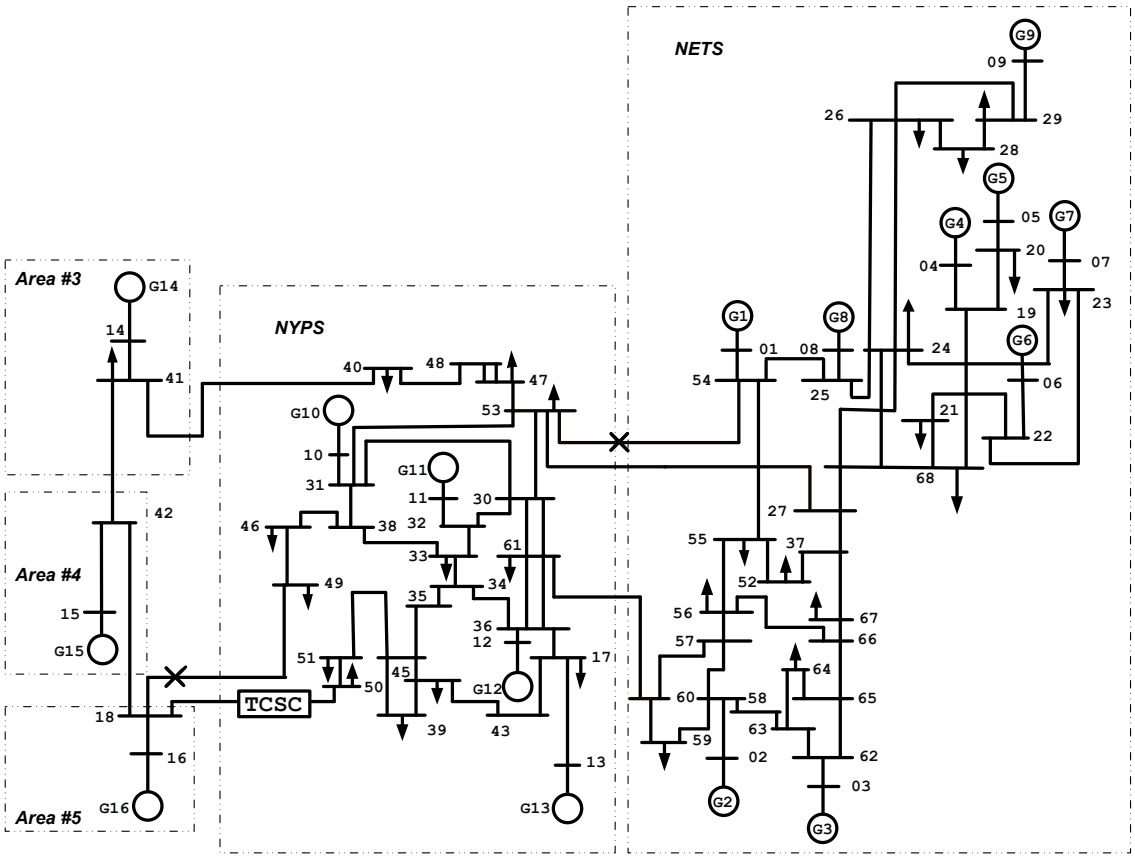

Figure 4: 16-machine, 5-area test system with a TCSC. Real power flow between buses 16 and 18 is used as feedback signal.

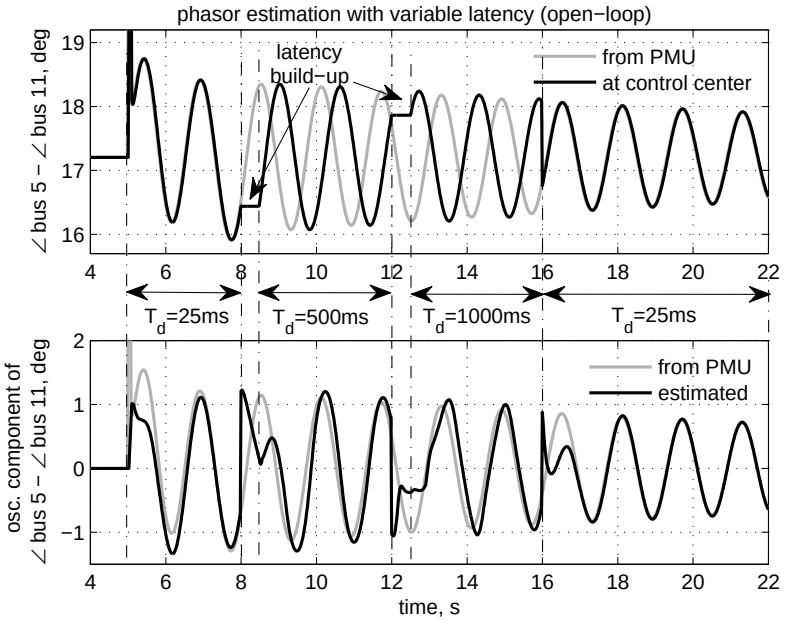

Figure 5: Response with a self-clearing fault near bus 8 (see Fig. 3). Grey trace (upper figure): Remote signal measured at PMU locations. Black trace (upper figure): Remote signal received at the control centre with variable latency (T_d) as marked. Grey trace (lower figure): Oscillatory component of the PMU measurements. Black trace (lower figure): Estimated oscillatory component after delay compensation.

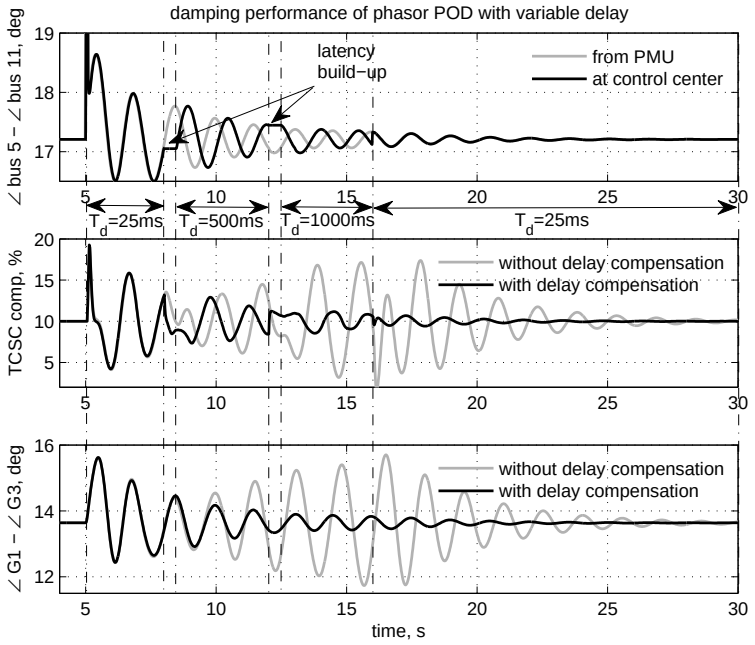

Figure 6: Closed loop system dynamics with a self-clearing fault near bus 8(see Fig. 3). Grey trace (upper figure): Remote signal measured at PMU locations. Black trace (upper figure): Remote signal received at the control centre with variable latency (T_d) as marked. Grey Trace (middle figure & lower figure): response without delay compensation. Black trace (middle figure & lower figure): response with delay compensation.

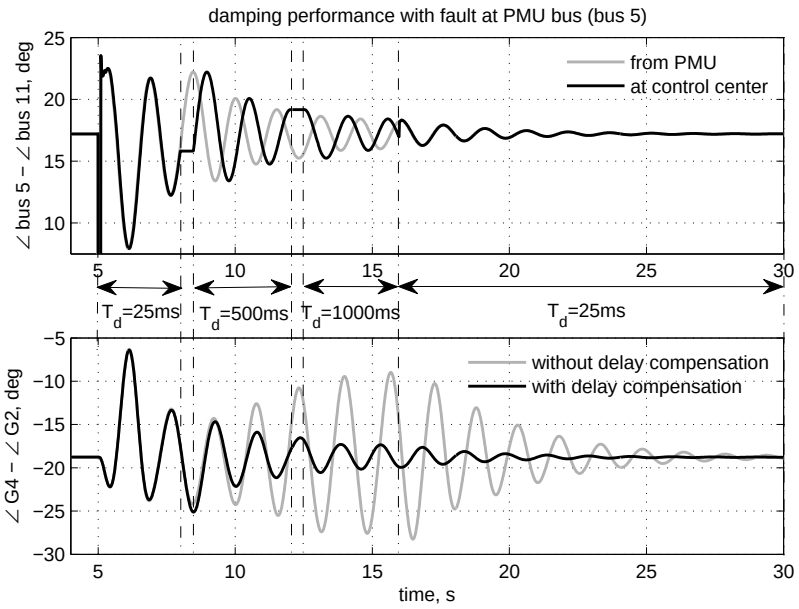

Figure 7: Damping performance with a self-clearing fault near bus 5 (PMU bus: see Fig. 3). Grey trace (upper figure): Remote signal measured at PMU locations. Black trace (upper figure): Remote signal received at the control centre with variable latency (T_d) as marked. Grey Trace (lower figure): response without delay compensation. Black trace (lower figure): response with delay compensation.

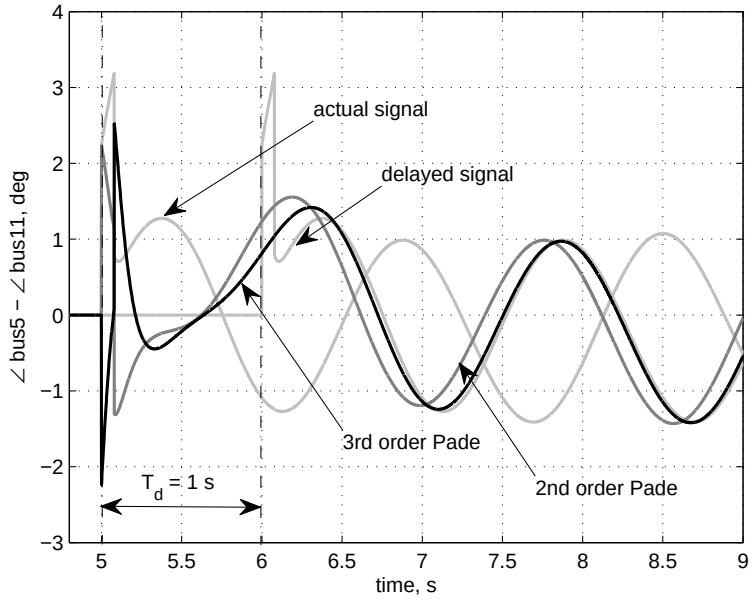

Figure 8: Effect of different Pade order approximations.

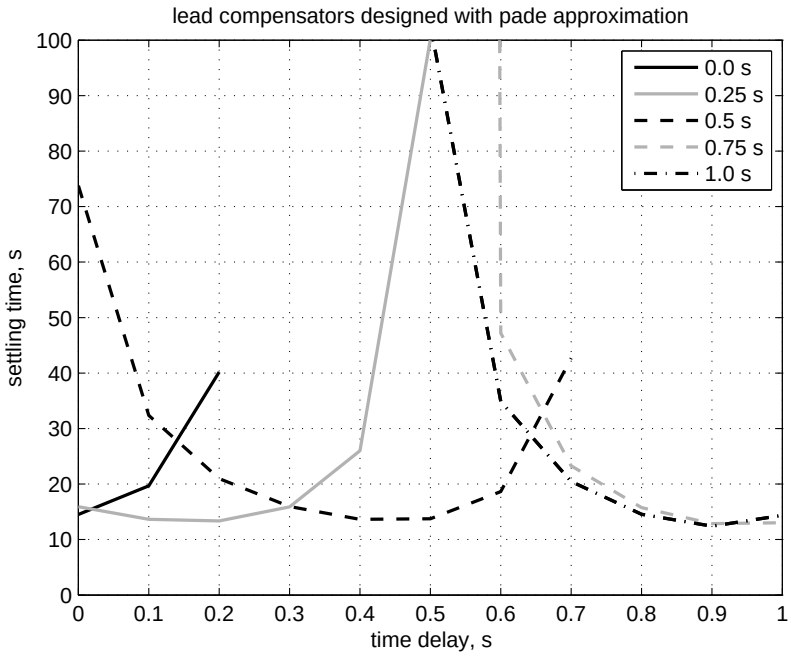

Figure 9: Lead compensators designed for desired closed loop performance in presence of signal latency - modelled by Pade approximation (e.g. Grey trace considers a latency of 250 ms). The effect on the settling time for a range of signal latency is illustrated.

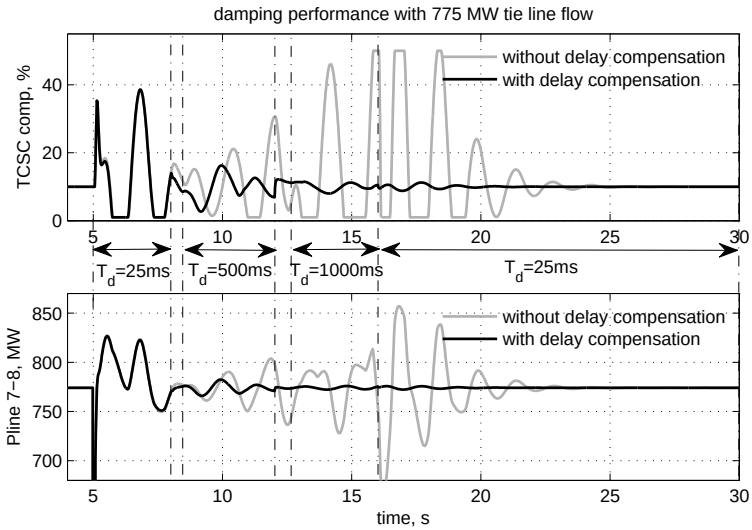

Figure 10: Damping performance with 775 MW tie-line flow after a self-clearing fault near bus 8(see Fig. 3). Grey trace: damping performance without delay compensation. Black trace: response with delay compensation.

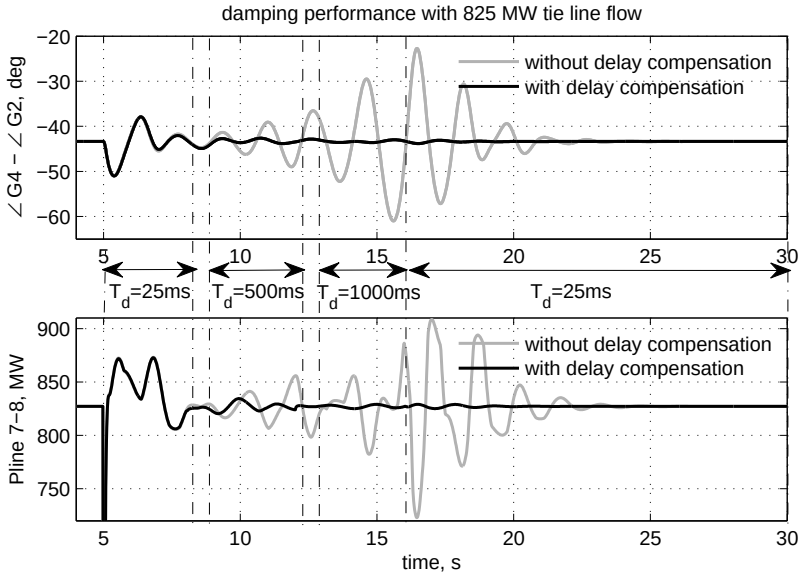

Figure 11: Dynamic behaviour with very high system loading (825 MW tie-line flow: see Fig. 3). Grey trace: damping performance without delay compensation. Black trace: response with delay compensation.

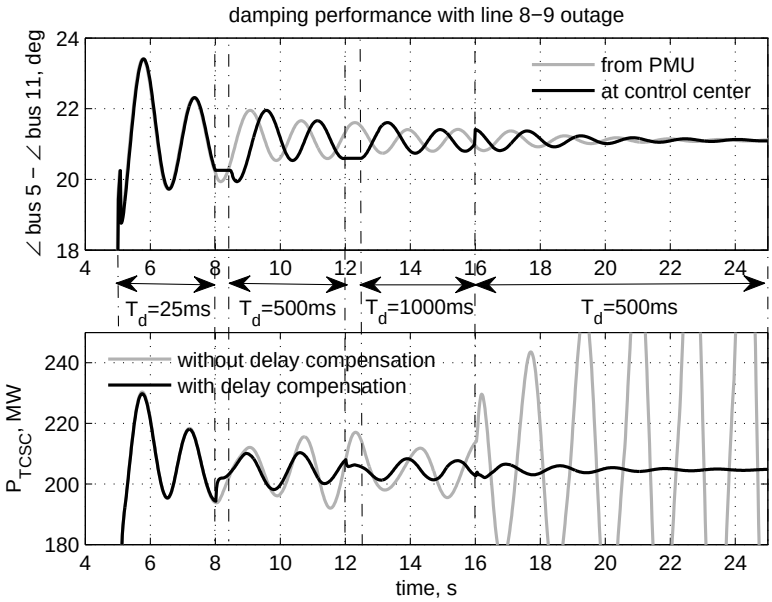

Figure 12: Response with fault near bus 8 followed by line 8-9 outage(see Fig. 3). Grey trace (upper figure): Remote signal measured at PMU locations. Black trace (upper figure): Remote signal received at the control centre with variable latency (T_d) as marked. Grey Trace (lower figure): TCSC line power flow without delay compensation. Black trace (lower figure): response with delay compensation. The system is unstable without delay compensation due to a sustained latency of 500 ms.

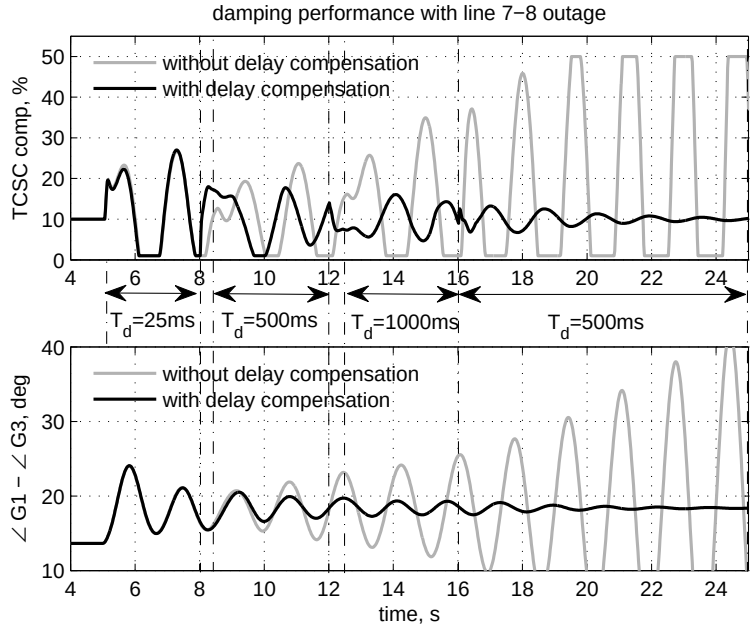

Figure 13: Damping performance with fault near bus 8 followed by line 7-8 outage(see Fig. 3). Grey trace : response without latency compensation. Black trace : response with delay compensation. The system is unstable without delay compensation due to a sustained latency of 500 ms.

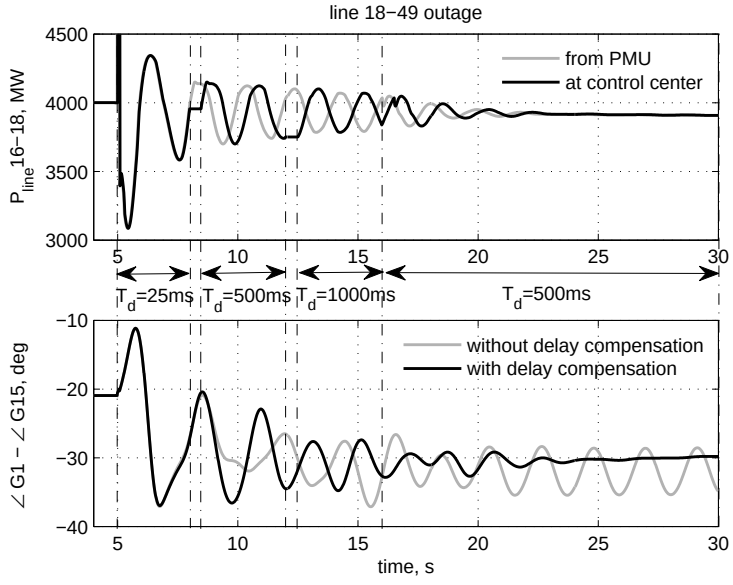

Figure 14: Damping performance with fault near bus 18 followed by line 18-49 outage(see Fig. 4). Grey trace (upper figure): Remote signal measured at PMU locations. Black trace (upper figure): Remote signal received at the control centre with variable latency (T_d) as marked. Grey Trace (lower figure): response without delay compensation. Black trace (lower figure): response with delay compensation.

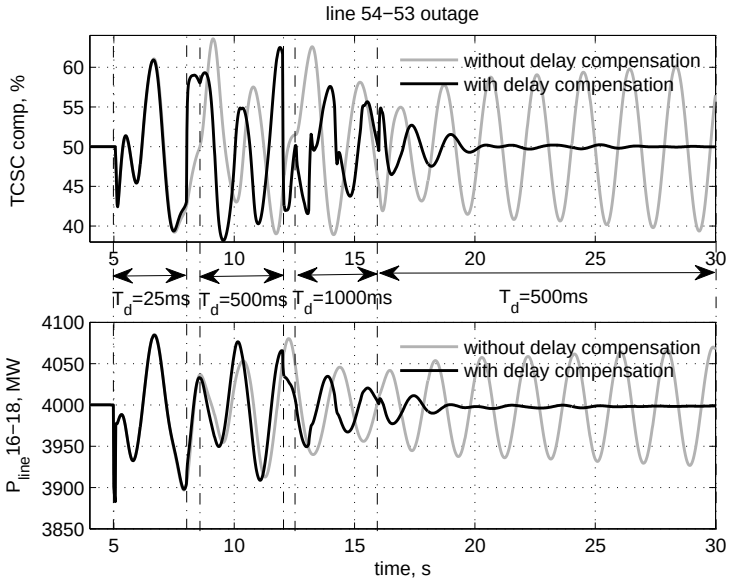

Figure 15: Damping performance with fault near bus 54 followed by line 54-53 outage(see Fig. 4). Grey trace: response without latency compensation. Black trace: response with delay compensation.